SCREEN CAPACITY

A force balance model of pulp screen capacity

D. MARK MARTINEZ, ROBERT W. GOODING, AND NORMAN ROBERTS

ABSTRACT

A screen capacity model can result by assuming that screen blinding limits volumetric capacity and that blinding occurs when a fiber floc becomes immobilized in a screen slot. The essential analysis is a force balance on a single floc in a slot with the forces arising from the flow through the slot, friction of the floc against the slot wall, and the rotor pulsations. The analysis gives an expression for capacity using hardware and pulp variables. Pilot plant trials with nine industrial screen plates determined constants for the analysis and verified the form of the equation.

Application:

A theoretical model uses pilot plant measurements of pulp screen capacity to identify the factors that limit capacity.

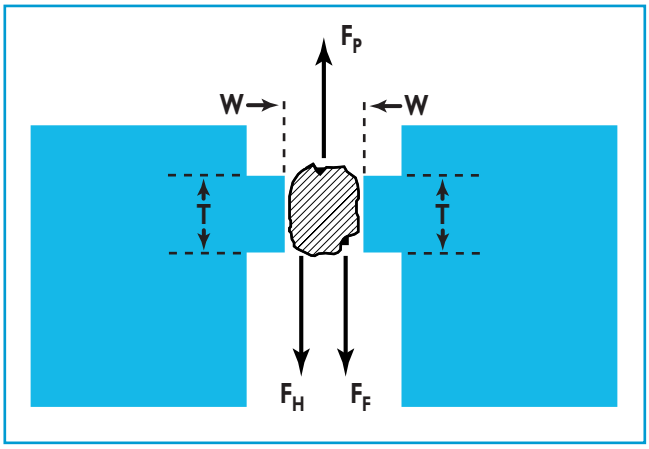
REDUCED SLOT WIDTH HAS BEEN the goal of many recent developments in pulp screen technology. Smaller slots can provide dramatic increases in removal of oversize contaminants. Increased removal efficiency helps to meet various challenges presently facing the pulp and paper industry. Competition in world markets dictates that industry provide a clean, high-quality product. Simultaneously, more widespread use of recycled fiber has increased the amount and variety of contaminants in the mill furnish. Environmental concerns with chlorine bleaching have limited its use for contaminant removal. Pulp screening with small slots has emerged as a technology that promises to satisfy these important and sometimes conflicting demands.

Methods of increasing screen capacity are essential to using small slots because they offset capacity losses that would otherwise accompany reduced slot width. The development of screen plate contours has been especially important in making small slots practical. Contours are depressions or protrusions on the feed side of the screen plate surface. Various contour shapes are available commercially, and several reports describe industrial applications *(1–3)*. Fundamental studies have identified mechanisms that underlie the action of screen contours. For example, contours can reduce the hydraulic resistance of a screen plate by streamlining the flow through it *(4, 5)*. Greater flows can therefore result from the same feed-accept pressure drop. A more streamlined flow may also increase passage of fibers through the screen to the accept stream. This would increase the accept consistency and total tonnage passed by the screen *(6, 7)*. Contours may also reduce accumulation of fibers in the slot that obstruct the flow. This may be due to the higher levels of turbulence at the slot entry and flow patterns that reduce fiber accumulation on the downstream edge of the slot entry *(5, 8)*.

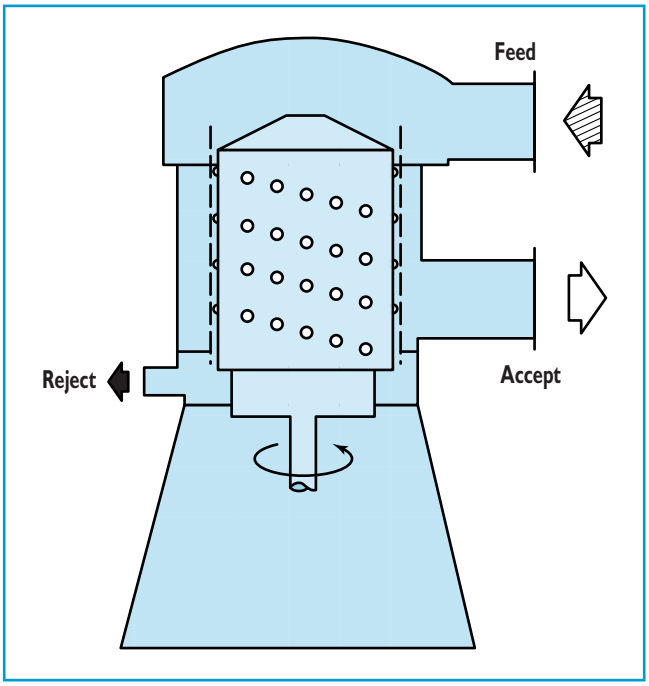
Improved design of the screen rotor is also an important factor for increasing capacity and using smaller screen slots. Screen rotors generate pressure pulsations that flush the slots and clear any accumulated fiber. Without clearing, screen plate blinding will occur, and the screen will fail, i.e., the accept flow from the screen will stop. Blinding is not the only way that a pulp screen can fail. Failure can also occur due to motor overloads, reject line plugging, or other phenomena, but blinding is probably the most common mode of failure for small slots.

Some novel rotors provide stronger and more effective pulses, and other rotors reduce thickening within the pulp screen *(9–11)*. Thickening is an increase in the pulp consistency on the feed side of the screen plate. It occurs as the pulp moves from the screen inlet to the reject outlet and the lower consistency accept flow is drawn through the screen plate. Pulp thickening leads to very high consistencies near the reject outlet and a greater tendency for slots in this region to blind. Rotors that generate strong pulses or reduce thickening support the use of screen plates with small slots. Screen plate contours and improved rotor designs have led to a threefold reduction in the minimum slot width used in industry from 0.50 mm to 0.15 mm during 1985–1995.

As discussed above, research studies have examined some specific mechanisms underlying the performance of improved screen plate rotor design. A comprehensive model of how these different mechanisms work together to determine capacity and the minimum slot size in pulp pressure screens does not exist. Such a model would examine the relative importance of hardware and pulp variables. This understanding is necessary for further development of screening technology and additional reductions in slot width. It is the subject of this study.



1. Forces applied to a floc in a slot in a screen plate [The mean flow through the screen plate is from the feed side (above) to the accept side (below).]



2. Schematic of pressure screen used in this study

The study begins with a mechanistic description of screen plate blinding. A mathematical model comes from the analysis to identify the factors that determine pulp screen capacity. The paper then describes pilot plant tests for a range of screen plates. Equations from the model were fit to the results of those tests, and the trends compared with experimental results. The combined theoretical and experimental findings describe which screen plate designs have the highest capacities and why.

ANALYSIS

The definition of screen blinding used here is the condition where fibers have become lodged in the screen slots and substantially limit the flow through the screen plate. When blinding occurs, the action of the rotor is no longer sufficient to flush backward and clear the slots. In industry, screen blinding is usually sensed from the pressure drop between the screen's feed and accept lines. This increases dramatically as the screen plate becomes obstructed *(12)*. Several types of blinds have been identified in the industry. A partial blind is the case where only some screen slots have become blinded. They are typically near the reject outlet where consistency is highest. A full blind means blinding of all screen slots. A slow blind or fast blind is distinguished by the rate at which a partial blind becomes a full blind. Regardlesss of the type of blind, the fundamental event is the obstruction of a slot with a fiber floc. The analysis that follows is based on a single slot.

The fiber floc that becomes lodged in the screen slot may have been created in the flow upstream of the slot. Flocs form in pulp suspensions at consistencies typically found in pulp screens: 1%–3%. Shear flows created by the rotor and screen contours may disrupt the fiber flocs and fluidize the pulp suspension. Alternatively, the stuck floc may form within the contour or screen slot itself from an accumulation of fibers. The origin of the fiber floc probably influences the floc's physical properties such as size, density, and compressibility. Origin of the floc should not have a strong bearing on the form of this analysis. The key point is that flocs have led to binding. That is evident from examination of a blinded screen plate.

The first step in the analysis is to conduct a force balance on a fiber floc lodged in the slot as **Fig. 1** shows. Three different forces affect the floc:

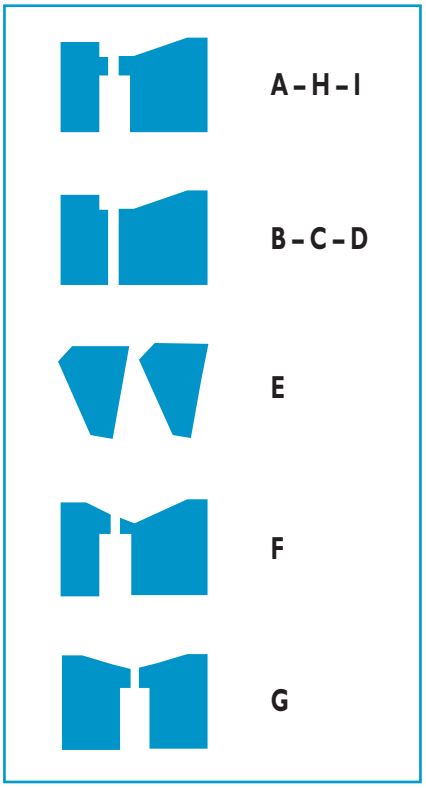
- Hydrodynamic force, F_H, arising from the pressure differential across the screen plate
- Pulsation force, F_p, associated with the pressure pulse from the rotor
- Frictional force, F_F, between the floc and the walls of the screen slot.

The hydrodynamic force tends to push the floc through the slot to the accept side of the screen plate. Conversely, the pressure pulse pulls the floc back to the feed side of the screen plate. The frictional force resists motion in either direction. Static equilibrium defines the condition when no net force acts to dislodge the fiber floc and blinding begins:

$$F_F = F_P - F_H \qquad (1)$$

The following equations approximate these forces per unit length:

$$F_F = 2\mu\sigma T \qquad (2)$$



3. Contour shapes for the screen plates in these trials (The direction of the rotor and the associated flow is from left to right. Dimensions are not to scale.)

$$F_P = P_P W \qquad (3)$$

$$F_H = \Delta P_{CR} W \qquad (4)$$

where
μ = the static coefficient of friction
σ = the compressive stress in the floc
T = the throat length in Fig. 1
W = the slot width in Fig. 1
P_P = the magnitude of the suction pressure of the rotor pulse
ΔP_{CR} = the critical pressure drop across the screen plate above which blinding occurs.

Gooding (4) studied the relationship between pressure drop and average slot velocity, and expressed the pressure drop across the screen plate, ΔP, in terms of the hydraulic resistance, K_H, and density of the suspension, ρ:

Plate	W, mm	T, mm	Slot length, mm	Slot spacing, mm	Slots/ plate	A, $m^2/10^{-3}$
A	0.22	0.8	55	3.2	1332	16.1
B	0.10	2.6	222	3.2	377	8.4
C	0.20	2.6	259	3.2	325	16.8
D	0.20	6.3	55	3.2	1649	18.1
E	0.20	0.6	319	3.2	377	24.1
F	0.20	0.6	45	5.1	942	8.5
G	0.20	0.8	53	3.2	1333	14.1
H	0.15	0.8	53	3.2	1319	10.5
I	0.20	0.6	255	3.2	377	19.2

I. Screen plate dimensions

$$\Delta P = K_H(\rho V^2/2) \qquad (5)$$

The maximum velocity through the slot, V_{MAX}, occurs when $\Delta P = \Delta P_{CR}$. The volumetric capacity of the screen plate, Q_{MAX}, then results by substituting Eqs. 2–5 into Eq. 1, rearranging, and multiplying V_{MAX} by the open area of the screen plate, A:

$$Q_{MAX} = A(2/\rho K_H)^{1/2}[P_P - 2\mu\sigma(T/W)]^{1/2} \qquad (6)$$

Equation 6 shows that three factors determine capacity: an area term, a resistance term, and a force term. Open area of the screen plate is easily measurable. The density of the suspension is assumed equal to that of water. The value of K_H depends on the slot width, contour shape, etc., and requires experimental assessment for each screen plate. Gooding (4) found that the relationship between K_H and V had a descending-constant form. A mathematical expression for the form of this relationship is the following:

$$K_H = a + b/V \qquad (7)$$

where
a and b = empirical constants.

The values of T and W can be measured directly, but accurate values of P_P, σ, and μ are not available. These values were instead determined by regression from pilot plant experiments using nine screen plates with a range of values for T/W. For this purpose, rearrangement of Eq. 6 gives the following:

$$K_H V_{MAX}^2 = 2P_P/\rho + [(-4\mu\sigma/\rho)(T/W)] \qquad (8)$$

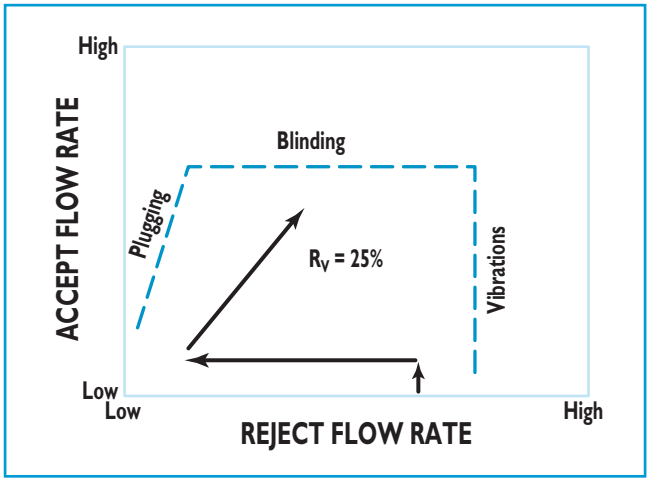
where
$K_H V_{MAX}^2$ = the dependent term
T/W = the independent term.

The pilot plant experiments estimated the slope, $(-4\mu\sigma/\rho)$, and intercept, $2P_P/\rho$, in Eq. 8 and tested the form of Eq. 6.

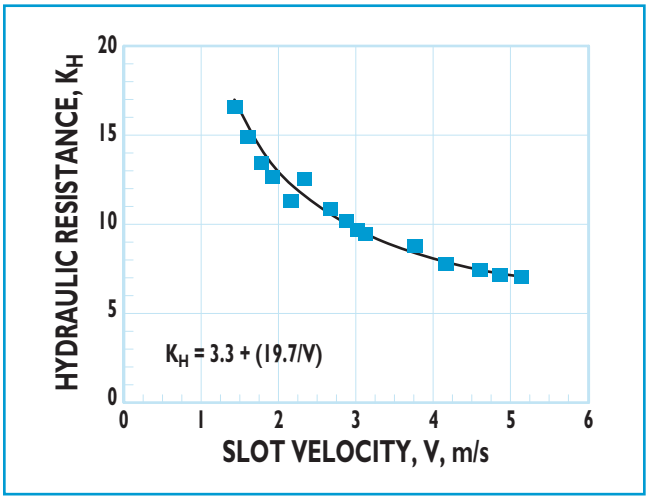
EXPERIMENTAL

Tests of screen capacity used a commercially available pressure screen in the PAPRICAN pilot plant. The screen shown in **Fig. 2** is a small, industrial-scale screen with a nominal capacity of 100 tons/day. It had a bumped rotor and operated at a rotor speed of 1700 rpm (30 m/s tip speed) for all the tests. A 55 kW motor drove the rotor. The study used nine screen plates that differed in slot spacing, slot width, contour design, and throat length. **Figure 3** shows the different screen contours, and **Table I** gives their dimensions.

The pilot plant has a distributed control system that controls the motors and valve positions. Measurements of flow rate, pressure, and motor load were recorded at 1 s intervals with a dedicated data acquisition system. Flow measurement used pulsed dc magnetic flow meters on the feed, accept, and reject lines. Feed, accept, and reject pressure measurements used capacitance-diaphragm transmitters on the lines leading to and from the pulp screen. Motor load measurement used an amperage current transformer calibrated for phase correction.



4. Test path for pilot plant trials



5. The K_H vs. V data for plate C typify the very good match obtained for the experimental data and the form of Eq. 7

Trial procedure

The trials used a 2% consistency reslushed softwood chemithermomechanical pulp (CTMP). The pulp had a freeness of about 80 mL, average fiber length of 2.1 mm (Kajaani length-weighted), and coarseness of 0.32 mg/m. The trial protocol began with the accept valve fully closed and the pulp suspension passing directly to the reject line at a flow rate of approximately 800 L/min. Feed pressure, P_F, was then adjusted to a value of 200 kPa that was maintained throughout the trial. Accept flow gradually increased and reject flow decreased until $R_V = 0.25$, where R_V is the volumetric reject ratio, i.e., the reject flow rate divided by the feed flow rate. The accept flow then increased while maintaining the target values of R_V and P_F until screen failure occurred.

Figure 4 shows this test path with the modes of failure that define the operating envelope of a pulp screen. This particular test path is such that the screen reaches its typical operating range without passing near regions where the reject ratio was low, reject consistencies would be high, and the thick pulp might cause premature screen blinding. Maintaining a constant reject ratio after passing through the typical operating range was an attempt to maintain a constant level of reject thickening. This was not perfect since the higher slot velocities reduce thickening.

The control limit for screen operation was a feed-accept pressure drop, ΔP_{CL}, of 120 kPa. The control system stopped flow to the screen at this value. The value of ΔP_{CR} was the maximum pressure drop for stable screen operation and is less than ΔP_{CL}. For all tests, the screen ran without dilution flow.

Plate	W, mm	a	b, m/s	K_H @ V = 2 m/s	ΔP_{CR}, kPa
A	0.22	1.1	35.4	18.8	65
B	0.10	9.7	50.1	34.8	40
C	0.20	3.3	19.7	13.1	60
D	0.20	2.9	21.9	13.9	100
E	0.20	4.7	24.1	16.8	110*
F	0.20	0.4	31.3	16.0	60
G	0.20	1.5	42.8	22.9	100
H	0.15	5.8	25.9	18.7	60
I	0.20	6.8	5.1	9.4	90

*The pumping capacity of the system not blinding limited plate E.

II. Screen plate resistance

RESULTS AND DISCUSSION

The specific objectives of the pilot plant experiments were the following:

- Assess the hydraulic resistance of each screen plate
- Measure the flow rate and pressure drop at which blinding occurred.

The following text presents the findings from each part of the work and discusses them in the context of the theory developed previously.

Assessing hydraulic resistance

As discussed above, the hydraulic resistance of a screen plate is characterized by the constants a and b of Eq. 7. Estimation of these constants used measurements of pressure drop between the feed and accept lines, ΔP, determined over a range of slot velocities, V, during normal screen operation, i.e., before the screen failed. Combining Eqs. 5 and 7 gives the following:

$$\Delta P = 0.5\rho(aV^2 + bV) \quad (9)$$

The constants a and b were estimated by regression of Eq. 9. Table II lists the results for each screen plate with the estimated value of K_H at V = 2 m/s, a constant value for all screens. Figure 5 compares the form of Eq. 7 to experimental data for

Plate	W, mm	Area term, $A, m^2 \times 10^{-3}$	Resistance term, $(2/\rho K_H)^{1/2}, m^{1.5}/kg^{0.5} \times 10^{-3}$	Force term, $[P_P - 2\mu\sigma(T/W)]^{1/2}, kg^{0.5}/m^{0.5}s$	Q_{MAX}, L/min, estimated	Q_{MAX}, L/min, measured	V_{MAX}, m/s, measured
A	0.22	16.1 (1.00)	14.4 (1.00)	287 (1.00)	4000 (1.00)	4000 (1.00)	4.1
B	0.10	8.4 (0.52)	7.1 (0.49)	236 (0.82)	800 (0.21)	600 (0.15)	1.2
C	0.20	16.8 (1.04)	15.9 (1.10)	267 (0.93)	4300 (1.07)	5000 (1.25)	5.0
D	0.20	18.1 (1.12)	14.3 (0.99)	222 (0.77)	3400 (0.86)	4000 (1.00)	3.7
E	0.20	24.1 (1.50)	13.6 (0.94)	288 (1.00)	5700 (1.41)	7000* (1.75)	4.8
F	0.20	8.5 (0.53)	17.4 (1.21)	288 (1.00)	2600 (0.64)	1800 (0.45)	3.5
G	0.20	14.1 (0.88)	11.9 (0.83)	286 (1.00)	2900 (0.72)	3200 (0.80)	3.8
H	0.15	10.5 (0.65)	12.3 (0.85)	283 (0.99)	2200 (0.55)	1600 (0.40)	2.5
I	0.20	19.2 (1.19)	15.9 (1.10)	288 (1.00)	5300 (1.32)	5400 (1.35)	4.7

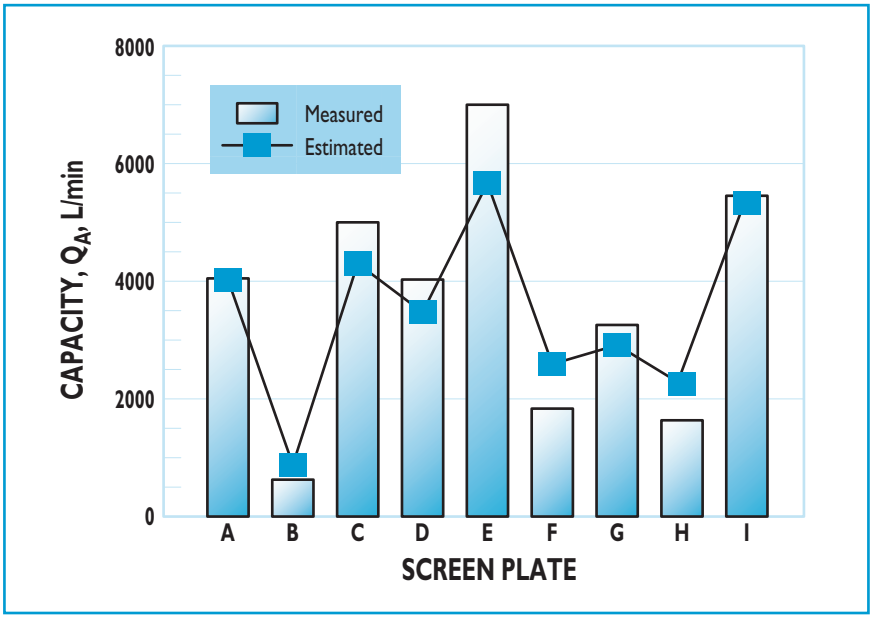
* The pumping capacity of the system not blinding limited Plate E.

III. Screen plate capacity

plate C and shows that the match is very close. Equally good fits resulted for the other screen plates. One must be cautious when using the values of a and b to characterize the screen plates in an absolute sense. The value of ΔP measured in these experiments includes the pumping effect of the rotor and the housing losses in addition to the pressure drop across the screen plate. The measured values of P_{CR} also include the pumping effect and housing losses, but these factors are assumed negligible for the small slot sizes used here *(4)*.

As Table II shows, plate I had the lowest or best value of K_H, and plates B and G had the highest values. The very small slot width in plate B was probably the reason for the very high resistance. Smaller slots do not intrinsically have a higher resistance *(4)*. Differences among the other plates probably resulted from contour shapes. These contours determine the amount of streamlining present and the tendency for fibers to obstruct the slot.

Table II also shows the critical pressure for each plate determined in the experiments. Some very low values are for plates with higher values of T, i.e., plates B and C. This is consistent with the above analysis since friction force increases linearly with T. Many contradictions also exist. Plate D has a high value of T and a high value of P_{CR}. Plate F has a low value of T and a low P_{CR}.



6. Comparison of experimental and theoretical measurements of capacity

A complete understanding of what determines P_{CR} is not yet available. Different contour designs probably give different degrees of pulp thickening. This increases density of the floc, the value of σ, and the friction with the slot wall. Alternatively, different slot contours may affect creation of the fiber floc, the character of the floc that enters the slot—size, compressibility, etc.—and the frequency at which flocs enter the slot. The present analysis begins with a floc in a slot and does not consider what happened before. Future studies that include these effects should provide additional insights into what determines P_{CR}.

Assessing capacity

Table III and **Figure 6** present the measured values of screen capacity for the screen plates in this study. The range of capacity, i.e., Q_{MAX} measured, is significant. It extends from 600 L/min for Plate B to 7000 L/min

for Plate E. Plate A is a common industrial screen plate and is the basis of comparison. The normalized capacities relative to Plate A vary from 0.15 to 1.75.

Although a comparison of screen plate capacity and the methodology of these tests has industrial interest, the larger goal of this study is to explain capacity differences. Eq. 6 does this by identifying the factorial groups that control capacity and the physical constants within the groups.

Table III shows the groups. As expected, the open area of the screen plate has a dominant influence on capacity. The plates with the greatest and least capacities (Plates E and B) have the greatest and least open areas. Area alone does not explain capacity. For example, Plate B has 52% of the open area of Plate A but only 15% of the capacity. Plate C has only 4% more area than Plate A but 25% more capacity. Other factors are obviously significant.

Table III also gives estimates of the resistance term using the data in Table II and Eq. 7. The values of the resistance term for plates B, G, and H were much lower than for plate A, i.e., hydraulic resistance was higher. This would help explain why the capacity of these plates was less than reduction in open area could explain. If capacity simply depended on open area, then the value of V_{MAX} would be the same for all plates. Consider that plate B has a V_{MAX} 0.29 times that of plate A and much of this reduction is due to the resistance term.

The third and final factor in this model of capacity is the force term associated with the release of flocs from the throat of the screen slot. As noted previously, accurate values for the constants in this term (P_p, μ, σ) are not available from the literature. They were therefore estimated by regression, i.e., by fitting the experimental values of $K_H V_{MAX}^2$ to T/W for the screen plates as given in Eq. 8.

The force term does not vary much for the range of slot widths and throat lengths in this study except plates B and D. The force term for plate B is 0.82 times that of plate A. Factoring this ratio with the ratios for the area and resistance terms indicates that the estimated ratio of capacity is 0.21. This is near the measured value of 0.15. One can also combine the area, resistance, and force terms for the other screen plates to obtain overall estimates of capacity. For most screen plates, the estimated values of capacity agree with the measured values within 20% as Table III shows. Figure 6 illustrates good agreement between the estimated and measured values of capacity.

Examining the values of P_p and σ derived from the regression constants in Eq. 8 also supports the validity of the above model. Assuming ρ = 1000 kg/m^3 and μ = 0.1 *(13)*, one obtains P_p of approximately 87 kPa and μ of approximately 6.0 kPa. These are generally consistent with published estimates *(4,14-17)*. This model is also consistent with industrial experience that shows screen capacity increases with increased temperature and reject ratio. Higher operating temperatures would lead to lower water viscosity and reduced values of K_H. Increased operating temperature would also reduce the stiffness of the fiber floc, reduce the frictional forces with the slot wall, and lead to increased capacity. The connection between reject ratio and capacity is probably because increased reject ratio will reduce the consistency near the reject outlet where blinding probably begins *(7)*. Lower consistencies are thought to produce a floc that is less dense or less stiff and has smaller frictional forces. Lower consistencies should also reduce the frequency of floc creation and the fiber hang-ups. This would decrease the effective open area of the screen plate.

SUMMARY AND CONCLUSIONS

Derivation of a force balance model of capacity for a pulp screen used the assumption that screens fail by blinding and that blinding occurs when frictional forces retain fiber flocs within screen slots. The model expresses capacity as the product of three terms: an area term, a resistance term, and a force term. These terms refer explicitly to common hardware and pulp variables such as slot width and suction pulse strength. The influence of other screening variables is expressed through constants in the equation. For example, pulp properties are reflected in the value of σ, and stock temperature affects the value of K_H.

Pilot plant measurements with nine industrial screen plates determined certain constants in the resistance and force terms. Using these constants, the model gave estimates that predicted the relative changes in capacity between the plates and supported the model validity.

The measurement of capacity for these screen plates has practical interest. A greater value of this work is providing a theoretical framework for understanding and ultimately increasing screen capacity. Previously, screen capacity could only be specified generally. This model allows equipment designers to identify opportunities for further equipment development. Mill personnel can use the model to investigate screen capacity problems and compare equipment options more objectively. What is perhaps most important is that the model will allow researchers to identify which constants have the greatest impact on capacity and assess the practical impact of their fundamental research findings.

Additional work remains in testing this model and expanding it to include various subordinate relationships such as the effect of temperature on K_H, the mechanism of floc creation, the influence of reject ratio

on screen capacity, and the effect of different rotor designs, i.e., different pulse forms. A need also exists for a more sophisticated model of blinding that does not assume equal velocities through all slots in the screen plate. Visualization studies would be useful to confirm the mechanism of blinding. The model described here does provide a useful beginning toward a general understanding of pulp screen capacity. **TJ**

Martinez is presently a research scientist at STFI, Stockholm, Sweden. Gooding (the corresponding author) is research engineer and Roberts is technical specialist at Paprican, 3800 Wesbrook Mall, Vancouver, BC V6T 2C1 Canada.

We gratefully acknowledge the support and technical advice of Frey Frejborg, Harold Earle, and James Olson in the conception and conduct of this study. CAE ScreenPlates Inc. provided the screen plates used in this study.

Received for review Oct. 20, 1997.
Accepted March 22, 1998.

NOMENCLATURE

A	screen plate open area, m^3
a	empirical constant
b	empirical constant, m/s
F_H	hydrodynamic force/unit len-gth, N/m
F_F	static frictional force/unit length, N/m
F_P	suction pulsation force/unit length, N/m
K_H	hydraulic resistance
P_A	pressure in accept line, kPa
ΔP	pressure drop across screen plate, kPa
ΔP_{CL}	control limit for pressure drop, kPa
ΔP_{CR}	critical pressure drop across screen plate, kPa
P_F	pressure in feed line, kPa
P_P	suction pulsation pressure, kPa
Q_{MAX}	volumetric capacity, L/min
R_V	volumetric reject ratio
T	thickness of the aperture throat, m
V	average slot velocity, m/s
V_{MAX}	maximum slot velocity, m/s
W	slot width, m
μ	static coefficient of friction
ρ	density of pulp suspension, kg/m^3
σ	compressive stress in floc, kPa

LITERATURE CITED

1. Boettcher, P. C., *TAPPI 1986 Pulping Conference Proceedings*, TAPPI PRESS, Atlanta, p. 279.
2. Frejborg, F., *Pulp Paper Can.* 89(1):107(1988).
3. Hooper, A. W., *Pulp Paper Can.* 90(5):47(1989).
4. Gooding R. W., "*The flow resistance of screen plate apertures,*" Ph.D. thesis, University of British Columbia, Vancouver, B. C., 1996.
5. Halonen, L., Ljokkoi, R., and Peltonen, K., *TAPPI 1990 Annual Meeting Proceedings*, TAPPI PRESS, Atlanta, p. 207.
6. Kumar, A., Gooding, R. W., and Kerekes, R. J., *TAPPI J.* 81(5):247(1998).
7. Gooding, R. W. and Kerekes, R. J., *Tappi J.* 75(11):109(1992).
8. Yu, C. J. and DeFoe, R. J., *Tappi J.* 77(8):219(1994).
9. Gallagher, B. J., *1994 CPPA Technical Section Pacific Coast and Western Branches Preprints*, CPPA, Montreal, p. 6.
10. Goldenburg, P. H., *1987 CPPA Annual Meeting Preprints*, CPPA, Montreal, p. B275.
11. Ernerfeldt, B. and Larsson, P. -E, *Svensk Papperstid.* 93(10):26(1990).
12. Gooding, R. W. and Craig, D. F., *Tappi J.* 75(2):71(1992).
13. Goncharov, V. N., *Bum. Prost.5:12(1971).*
14. Karvinen, R. and Halonen, L., *Paperi Puu* 66(2):80(1984).
15. Javid, S. R., *Pulp & Paper* 57(3):182(1983).
16. Martinez, D. M., Batchelor, W. J., Kerekes, R. J., *et al., J. Pulp Paper Sci.* 23(1):11(1997).
17. Yu, C. J., Crossley, B. R., and Silveri, L., *Tappi J.* 77(9):125(1994).